ADVANCED FUNCTIONAL MATERIALS
www.afm-journal.de

Self-Organization of Inkjet-Printed Organic Semiconductor Films Prepared in Inkjet-Etched Microwells

Donghoon Kwak, Jung Ah Lim, Boseok Kang, Wi Hyoung Lee, and Kilwon Cho**

The high-precision deposition of highly crystalline organic semiconductors by inkjet printing is important for the production of printed organic transistors. Herein, a facile nonconventional lithographic patterning technique is developed for fabricating banks with microwell structures by inkjet printing solvent droplets onto a polymer layer, thereby locally dissolving the polymer to form microwells. The semiconductor ink is then inkjet-printed into the microwells. In addition to confining the inkjet-printed organic semiconductor droplets, the microwells provide a platform onto which organic semiconductor molecules crystallize during solvent evaporation. When printed onto the hydrophilic microwells, the inkjet-printed 6,13-bis(triisopropylsilylethynyl) pentacene (TIPS_PEN) molecules undergo self-organization to form highly ordered crystalline structures as a result of contact line pinning at the top corner of the bank and the outward hydrodynamic flow within the drying droplet. By contrast, small crystallites form with relatively poor molecular ordering in the hydrophobic microwells as a result of depinning of the contact line along the walls of the microwells. Because pinning in the hydrophilic microwells occurred at the top corner of the bank, treating the surfaces of the dielectric layer with a hydrophobic organic layer does not disturb the formation of the highly ordered TIPS_PEN crystals. Transistors fabricated on the hydrophilic microwells and the hydrophobic dielectric layer exhibit the best electrical properties, which is explained by the solvent evaporation and crystallization characteristics of the organic semiconductor droplets in the microwell. These results indicate that this technique is suitable for patterning organic semiconductor deposits on large-area flexible substrates for the direct-write fabrication of high-performance organic transistors.

1. Introduction

Inkjet printing has received considerable attention in an effort to control the deposition of small amounts of organic semiconductors and other functional materials.[1,2] Inkjet printing may be applicable to large-area/high-throughput processes as well as flexible substrates for the fabrication of flexible electronics. Inkjet printing of soluble organic semiconductors has been intensively investigated, for example, for fabricating organic thin film transistors (OTFTs).[3–5] The surface energy of a substrate and the spreading and drying behavior of the ink critically affect the position and morphology of the resulting printed droplet, thereby influencing the electrical properties of an OTFT fabricated using printed semiconductor deposits. The pattern accuracy may be increased by steering the ink spreading using local patterns on the substrate surface. One approach involves prepatterning banks of insulator materials onto the substrate to concentrate the ink into defined areas.[6,7] Prepatterning processes, however, have unfortunately presented an obstacle to the production of large-area displays: prepatterning processes rely on conventional photolithographic techniques that are complicated and relatively costly.

This letter describes a technique for preparing surface patterns by inkjet printing organic solvent droplets onto an insulator film to form microwells. This technique does not suffer from the disadvantages of photolithographic techniques. Small solvent droplets can locally etch away a thin polymer film, and the resulting microwells have been used to produce interconnections between functional layers in organic transistor circuits.[8] Here, we demonstrate that inkjet-etched microwells can also be used to build prepatterned "banks" that can confine inkjet-deposited semiconductor droplets to facilitate the high-throughput fabrication of organic transistors.[9,10]

High-performance organic devices rely on the preparation of inkjet-printed organic semiconductor films with uniform morphologies and desirable crystalline microstructures.[11,12] In recent years, the evaporation characteristics of inkjet-printed droplets on a flat surface have been studied in an effort to control the morphologies and microstructures of the dried

Dr. D. Kwak,[+] B. Kang, Prof. K. Cho
Department of Chemical Engineering
Pohang University of Science and Technology
Pohang 790–784, Korea
E-mail: kwcho@postech.ac.kr
Dr. J. A. Lim
Future Conversions Research Division
Korea Institute of Science and Technology
Seoul 130–650, Korea
Prof. W. H. Lee
Department of Organic and Nano System Engineering
Konkuk University
Seoul 143–701, Korea
E-mail: whlee78@konkuk.ac.kr
[+]Present address: Display Research Center, Samsung Display, Yongin, Gyeonggi-do 446–771, Korea

DOI: 10.1002/adfm.201300936

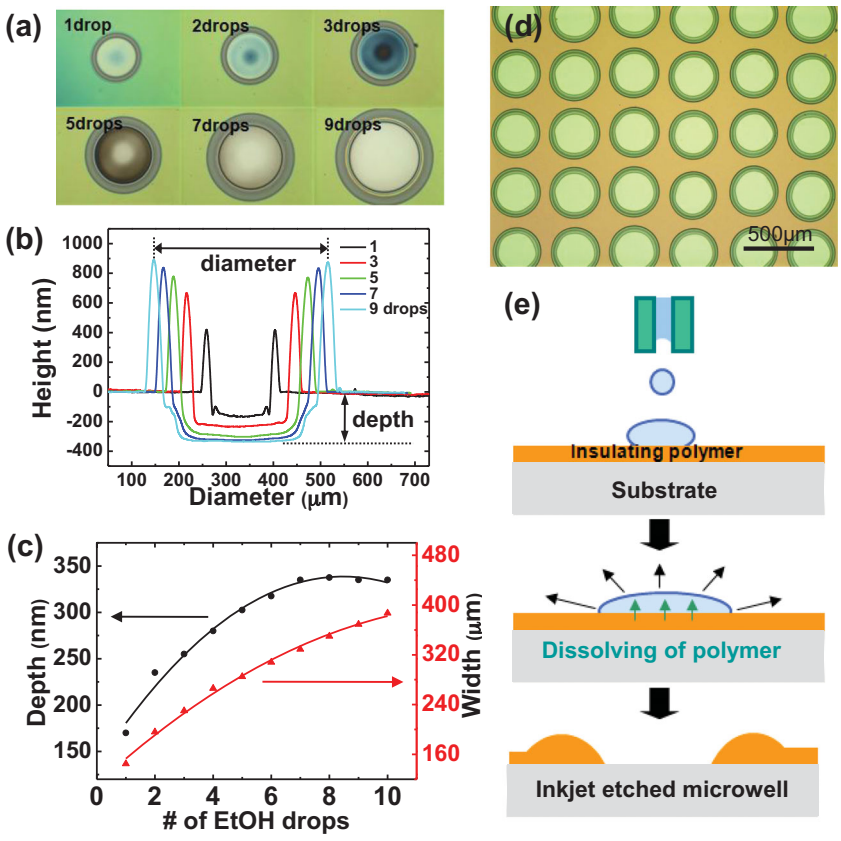

Figure 1. a) Optical microscopy (OM) images and b) height profiles of the inkjet-printed PVP microwells, as a function of the number of inkjet-printed ethanol drops. c) The depth and diameter of the PVP microwells increased with the number of ethanol drops. d) OM image of the microwells patterned by inkjet printing. e) Schematic diagram showing the formation of the crater-like inkjet etched microwell structures.

deposits.[13,14] The evaporation properties of the droplets depend on the ink composition, the surface properties of the substrate, and the environmental conditions.[3,15–20] In a previous study, we demonstrated the influence of the hydrodynamic flows in a drying droplet on the crystalline microstructures of printed organic semiconductors using a mixed solvent.[3] The surface wettability of the dielectric substrate can also affect the morphology and crystalline microstructure of an inkjet-printed organic semiconductor film;[20] however, the evaporation properties of inkjet-deposited droplets on a confined bank, such as a microwell structure, have not been extensively explored, and the influence of a microwell structure on the self-organization characteristics of printed organic semiconductors warrants examination.

In this study, we propose a facile method for fabricating microwells to form a prepatterned bank by inkjet printing solvents onto a thin polymer layer. The prepatterned bank was then used to prepare high-performance OTFTs. We systematically examined the evaporation properties of an organic semiconductor layer that had been inkjet-printed into the microwells of a prepatterned surface prepared to have a precisely tuned surface wettability. Two types of polymer surfaces were used to tune the wettability of the microwell-patterned surface: poly(vinyl phenol) (PVP) and poly(4-methyl styrene) (P4MS). 6,13-Bis(triisopropylsilylethynyl) pentacene (TIPS_PEN) was used as an organic semiconductor ink because it is solution processable and features efficient π-orbital overlap, yielding excellent charge transport characteristics.[21–23]

2. Results and Discussion

Well-defined microwell patterns were fabricated by depositing a small solvent drop onto the thin polymer film by inkjet printing.[24–26] The drops dissolved the polymer film and then re-deposited the polymer upon solvent evaporation. As the droplet containing the dissolved polymer dried, the polymer material was found to preferentially re-deposit at the contact line of the solvent drop (the edge of the sessile droplet). This resulted in a reduced polymer film thickness at the center of the droplet and the formation of a ridge at the edge. Repeated deposition of a solvent drop at a single position deepened the hole and increased the height of the ridge. Finally, a complete hole in the polymer layer remained, exposing the underlying substrate surface. The images in **Figure 1**a show holes with perfectly circular shapes formed by the sequential deposition of ethanol drops onto a PVP film. The change in the film thickness was apparent from the change in the interference color. The reflected color in the hole regions changed as the number of deposited drops increased (1–7 drops), and the color did not change beyond a certain number of solvent droplet deposition steps (7–9 drops). These results suggested that the thickness of the polymer layer at the bottom of the hole decreased as the number of solvent drops increased, eventually exposing the underlying substrate layer (SiO_2/Si), which was insoluble. The measured height profiles revealed that after drying of the solvent droplets, most of the polymer was redistributed around the perimeter of the hole, producing a thick edge and leaving almost no polymer inside the microwell (Figure 1b). Figure 1c shows the depth and diameter of a microwell as a function of the number of ethanol drops. The diameter of the printed microwell was approximately proportional to the number of drops, and the depth of the microwell formed by more than 7 drops of ethanol was found to be equal to the thickness of the polymer layer (350 nm). Energy dispersive spectroscopy (EDS) spectra, as shown in Supporting Information Figure S1, confirmed the absence of residual polymer molecules in the center region of the microwell. The patterned arrays of microwells on the substrate were prepared simply by depositing multiple solvent droplets in a regular manner (Figure 1d). These results confirmed that the inkjet technique is suitable for patterning arrays to prepare banks for use in printed circuits.

The mechanism underlying the formation of the microwells using the solvent drops differed from the mechanism

Table 1. Contact angles (CA) and surface energies of the polymer microwells (PVP, P4MS) and the dielectric layers prepared with different surface treatments (Bare, HMDS).

	Microwell material		Dielectric layer	
	PVP	P4MS	Bare	HMDS
Water CA (deg)	60	92	<5	70
Diiodomethane CA (deg)	27	31	<5	49
Surface energy[a] [mJm^{-2}]	50.3	44.6	287[b]	39.3
Tetralin CA [deg]	<5	16	<5	25

[a]The surface energies were determined from contact angle measurements performed using distilled water and diiodomethane as probe liquids, by applying the geometric mean equation: $(1 + \cos\theta)\gamma_{pl} = 2(\gamma_s^d\gamma_{pl}^d)^{1/2} + 2(\gamma_s^d\gamma_{pl}^d)^{1/2}$, where γ_s and γ_{pl} are the surface energies of the dielectric layer and the probe liquid, respectively, and the superscripts d and p refer to the dispersion and polar components of the surface energy; [b]The data were derived from ref. [32].

underlying conventional wet etching processes. In the conventional case, a bulk etchant will etch a material, which is then washed away by rinsing with a solvent. In the inkjet etching process, however, the polymer dissolved in a printed solvent drop first and then was subsequently transported by the capillary flow induced inside the droplet from the center region to the edge. The polymer finally re-solidified at the rim of the droplet. A ring-like deposit of solute formed during droplet drying via the "coffee-ring" effect. This effect results from conditions that produce a maximal evaporation rate at the outer edges of the droplet while the solvent edge remains pinned at the three-phase contact line. Pinning of the contact line during drying preserves the fixed contact diameter of the droplet such that the hydrodynamic flow of the solvent proceeds from the center of the droplet toward the contact line, thereby replenishing the solvent lost due to evaporation. The outward hydrodynamic flow transports the suspended solute to the drop's perimeter. The same mechanism governs the formation of a crater-like well structure (Figure 1e). Repeated deposition of solvent at a position then dissolves the remaining polymer in that deposition location, and the polymer is then transported to the edge of the droplet. Ultimately, all materials are removed from the central region.

The surface properties of the substrate significantly affected the evaporation properties of the inkjet-printed organic semiconductors and governed the final morphology and microstructure of the films.[20] We systematically examined the influence of the surface wettability of the prepatterned polymer microwells on the evaporation behavior of an inkjet-printed organic semiconductor. The surface wettability of the microwell was tuned according to the composition of the polymer layer: PVP (to produce a hydrophilic bank) or P4MS (to produce a hydrophobic bank, **Table 1**). The silicon oxide substrate surface was treated with UV-ozone plasma (Bare) or 1,1,1,3,3,3-hexamethyldisilazane (HMDS). A tetralin solution containing dissolved TIPS_PEN (1 wt%) was inkjet-printed onto the prepatterned polymer banks with different surface wettabilities. The morphologies of the inkjet-printed droplets of the TIPS_PEN deposited in the microwells are shown in **Figure 2**. In the case of the hydrophilic PVP microwell, TIPS_PEN crystals several tens of micrometers in diameter were observed with clear optical contrast (Figure 2a). This result indicated that the crystals consisted of uniaxially ordered polymer molecules within the crystals. By contrast, the hydrophobic P4MS microwells preferentially induced the formation of small crystallites at the edges of the microwell, whereas large crystals formed in the central region (Figure 2b). The TIPS_PEN crystals in the microwells were further characterized by field emission scanning electron microscopy (FESEM) imaging. Large crystals grew in the PVP microwells from the edges toward the center of the microwell. The cross-sectional view clearly shows that the crystals nucleated at the top corner of the microwell. On the other hand, the top and cross-sectional views of the P4MS microwell showed that

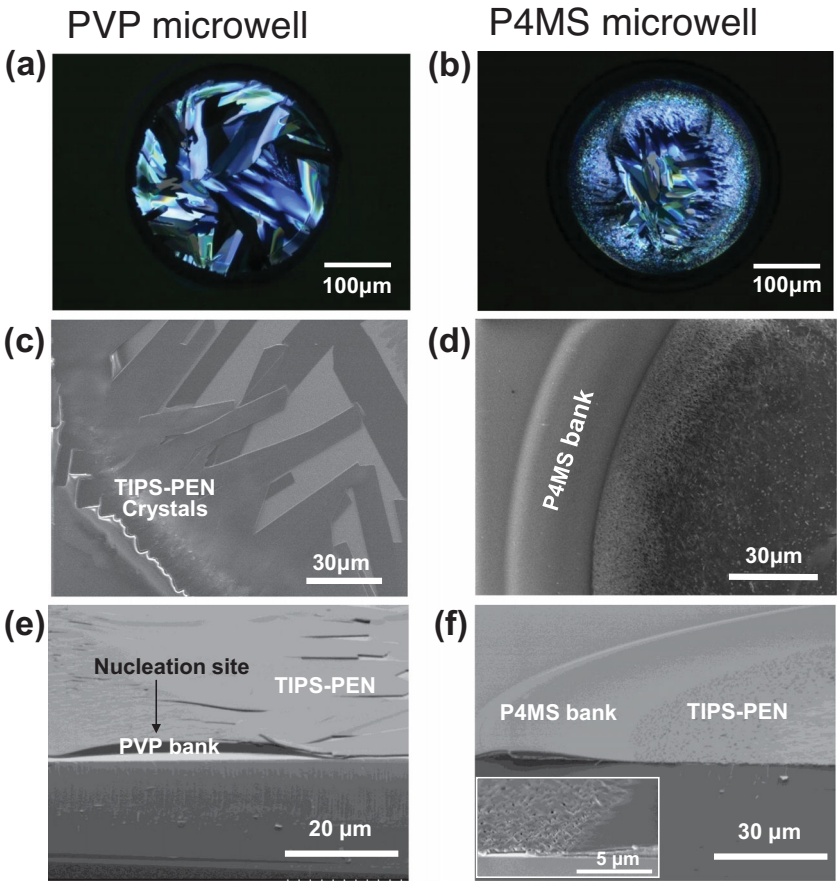

Figure 2. a,b) Polarized OM and c,d) SEM images of the TIPS-PEN deposited by inkjet printing onto the a,c,e) inkjet-patterned PVP microwells or the b,d,f) P4MS microwells. e,f) Cross-sectional views of the SEM images. All images were obtained on the Bare-dielectric sample.

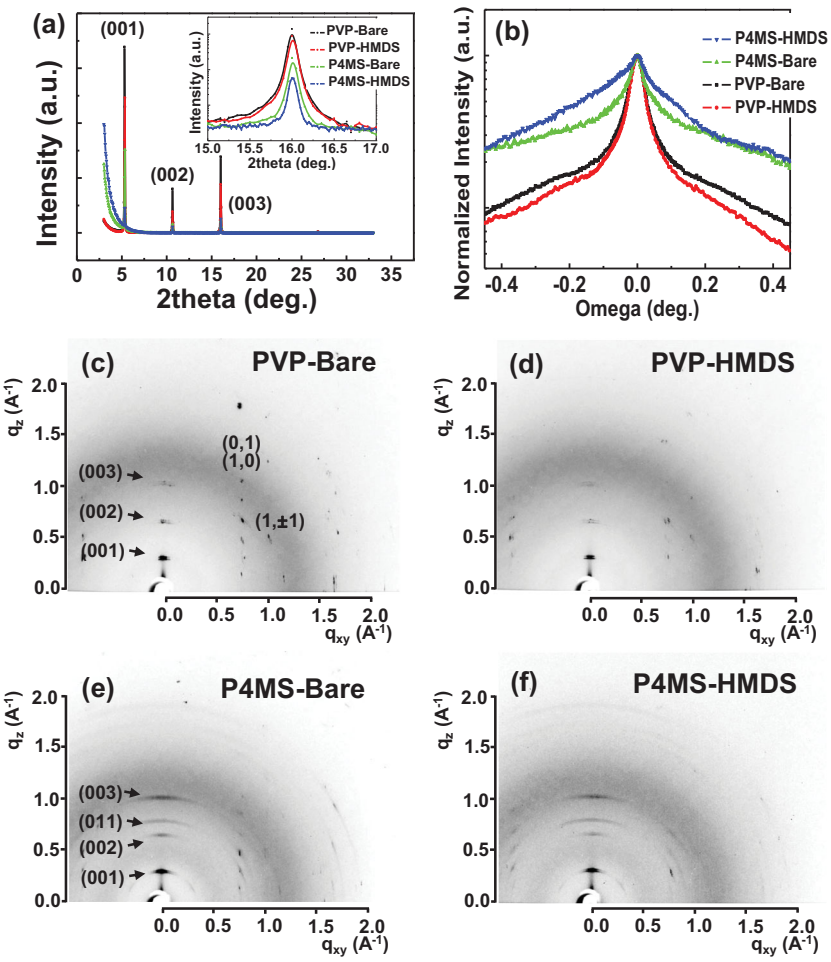

Figure 3. a) Out-of-plane XRD patterns (θ-2θ mode). The inset of (a) shows magnified plots of the (003) diffractions. b) Rocking curves for the (003) peak of the TIPS_PEN deposits prepared in each type of microwell (PVP or P4MS) and for each type of surface treatment (Bare or HMDS). c–f) 2D GIXD patterns for the TIPS-PEN deposits grown in microwells with different surface treatments: c) PVP-Bare, d) PVP-HMDS, e) P4MS-Bare, f) P4MS-HMDS.

small crystallites were deposited at the edges of the bottom surface inside the microwell.

The inner crystalline structures of the TIPS_PEN films were examined by analyzing the XRD patterns, as shown in **Figure 3**a. A given quantity of a TIPS_PEN solution (20 drops) was inkjet-printed into the microwells of diameter 400 µm to compare the diffraction patterns as a function of the microwell surface wettability. The diffraction spectra of these samples contained only (00*l*) reflections (Figure 3a) corresponding to a *c*-axis of 16.8 Å in the TIPS_PEN unit cell, which indicated that the TIPS_PEN molecules were oriented such that the silyl groups were arranged on the substrate surface; however, the peak intensities observed from the TIPS_PEN crystals grown in the hydrophobic P4MS microwells were weaker than those obtained from the hydrophilic PVP microwells. Rocking curves on the (003) reflections were obtained to measure the angular spread of the molecular orientations in the crystallites (Figure 3b). The (003) peak was chosen because the background reflection of the (003) diffraction was significantly weaker than that of the (001) diffraction. Each curve was normalized by the maximum value of the (003) peak. A small full-width at half-maximum (FWHM) value in the hydrophilic PVP microwells indicated that the TIPS_PEN crystals displayed a narrow distribution of molecular orientations. Regardless of whether the substrate surface was treated with HMDS, the crystals exhibited a large lateral coherence length associated with the (00*l*) planes. These results confirmed that the molecular orientations of the TIPS_PEN crystals formed in the PVP microwell depended largely on the nucleation behavior at the top corner of the microwell, rather than on the substrate surface conditions. By contrast, the molecular orientations of the TIPS_PEN crystals grown on surfaces without microwells depended largely on the surface energy of the substrate onto which the TIPS_PEN droplets were inkjet-printed.[20] In the hydrophobic P4MS microwells, however, the crystals displayed relatively broad distributions of the molecular orientations.

The molecular orientations in the inkjet-printed TIPS_PEN films were further investigated by 2D-grazing incidence X-ray diffraction (GIXD). The TIPS_PEN deposit grown in the PVP microwell yielded a diffraction pattern with many reflection spots in the direction of q_z (out-of-plane) at a given q_{xy} (in-plane), indicating that the TIPS_PEN film crystals were well-ordered in both the vertical and lateral directions (Figure 3c,d);[27] however, the diffraction patterns for the crystals grown in the P4MS microwells contained both (00*l*) reflections, corresponding to a c-axis of 16.8 Å in the TIPS_PEN unit cell, and an intense (011) peak along the q_z axis (Figure 3e,f).[22,23] This result suggested the existence of an unfavorable orientation among the TIPS_PEN molecules in the film state in which the pentacene ring of the TIPS_PEN molecule was stacked along a direction perpendicular to the surface. The angular spread of the (00*l*) reflections from crystals grown in the P4MS microwells was much larger than that observed in the reflections obtained from crystals grown in the PVP microwells. These results suggested that highly ordered TIPS_PEN crystals could be produced by inkjet printing via control over the surface wettability of the microwells.

Insight into the self-organization process by which the inkjet-printed TIPS_PEN droplets formed crystals in the microwells prepared with different surface wettabilities was sought by investigating the evaporation properties of the drying droplets. To this end, top view images of the drying process were recorded using a CCD camera. **Figure 4**a shows the morphological evolution of the inkjet-printed TIPS_PEN droplets in a hydrophilic PVP bank. Droplet evaporation proceeded in three distinct stages (see Figure 4b). During the initial stage,

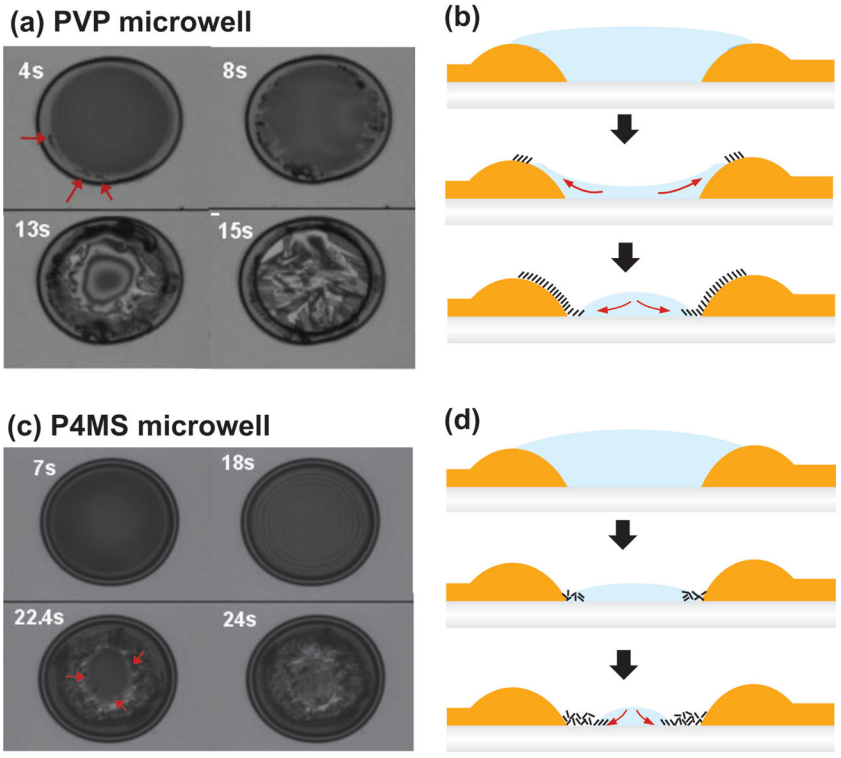

Figure 4. In situ time-resolved OM images of an evaporating TIPS_PEN droplet in each type of microwell, obtained from the vertical CCD camera: a) PVP and c) P4MS. Schematic diagrams of the TIPS-PEN droplet evaporation process for droplets that had been inkjet-printed into each type of microwell: b) PVP and d) P4MS.

the meniscus remained pinned at the top corner of the circular droplet perimeter; thus, the shape of the meniscus changed from a convex to a concave structure during prolonged solvent evaporation. As a result, the contact angle (measured by finding the line tangent to the intersection of the droplet with the surface) decreased.[28] During the second stage, nucleation of the TIPS_PEN crystals occurred at the top corner of the microwell wall, that is, the pinned contact line. Finally, the TIPS_PEN molecules self-assembled under the hydrodynamic flow, and the crystals aligned along a line formed from the top corner to the center of the microwell. In a previous report, we demonstrated that these observations may be explained in terms of a "drying-mediated self-assembly" process resulting from the outward hydrodynamic flows toward the pinned contact line.[20] The outward hydrodynamic flow resulting from contact line pinning transported the TIPS_PEN molecules from the center to the periphery of the droplet so that the concentration of TIPS_PEN at the contact line was higher than that in the interior region. Because the critical concentration required for nucleation was reached predominantly at the contact line rather than in the central region, nucleation preferentially occurred near the pinned contact line. The molecules supplied by the outward flow self-assembled from the nucleation site to the internal region of the droplet via intermolecular π–π interactions. Thus, highly crystalline TIPS_PEN crystals with preferential molecular orientations were obtained through controlled solvent evaporation in the hydrophilic PVP microwell (Figure 3).

In the hydrophobic P4MS microwell, the droplet meniscus in the P4MS bank was not pinned at the top of the well. Instead, the droplet edge moved downward during solvent evaporation (Figure 4c,d).[29,30] The continuous retraction of the droplet contact line in the hydrophobic wall prevented the establishment of an outward hydrodynamic flow in the drying droplet. Thus, the critical concentration needed to trigger crystal nucleation and growth was not reached. As drying proceeded, the molecules in the droplets condensed and small crystallites formed near the edges of the bottom substrate.[31] We therefore surmised that the contact line receded rapidly during the initial stages, and the TIPS_PEN crystals that formed in the hydrophobic microwells assumed unfavorable orientations, as confirmed by 2D-GIXD measurements (Figure 3e,f). The concentration of the TIPS_PEN in the droplet increased with the ink viscosity. The contact line could be pinned at the edge of the bottom substrate inside the microwell. This in turn allowed TIPS_PEN to crystallize in the center region; however, the sizes of the crystals in the P4MS microwells were not as large as those obtained in the PVP microwells because the high viscosity prohibited efficient transport and stacking of the TIPS_PEN molecules.

The relationship between the morphology, film structure, and electrical performance of these deposits in the context of inkjet-printed organic transistors was examined by fabricating closed-ring devices. Prior to patterning the source/drain electrodes, the gate dielectric layers were modified by UV-ozone treatment (Bare) and HMDS. Microwells (PVP or P4MS) were selectively formed onto the prepatterned source/drain electrodes using the positioning system of the inkjet printer. Finally, a TIPS_PEN solution (10 droplets) was inkjet-printed into the microwell. Self-aligned TIPS_PEN crystals with a highly ordered crystalline structure developed in the channel regions of the hydrophilic PVP microwell. Note that crystals nucleated at the top corner of the wall and grew by extending toward the center of the drain electrode (**Figure 5**a). Notably, because the morphology and crystallinity of the TIPS_PEN deposit depended on the surface wettability of the bank rather than the surface wettability of the substrate, well-ordered TIPS_PEN crystals were successfully obtained on the hydrophobic HMDS-treated SiO_2/Si substrate by using hydrophilic PVP microwells (Supporting Information, Figure S2). This result contrasts with results obtained from our previously fabricated FET devices on hydrophobic substrates prepared without a bank, which exhibited a dewetted TIPS_PEN deposit in the channel region due to the surface energy differences between the hydrophobic channel region and the electrode (Supporting Information, Figure S3). Enhanced device performances (i.e., a high field-effect mobility, a low threshold voltage, a low charge carrier trap density) are commonly reported from TFTs prepared on hydrophobic dielectric surfaces; therefore, the

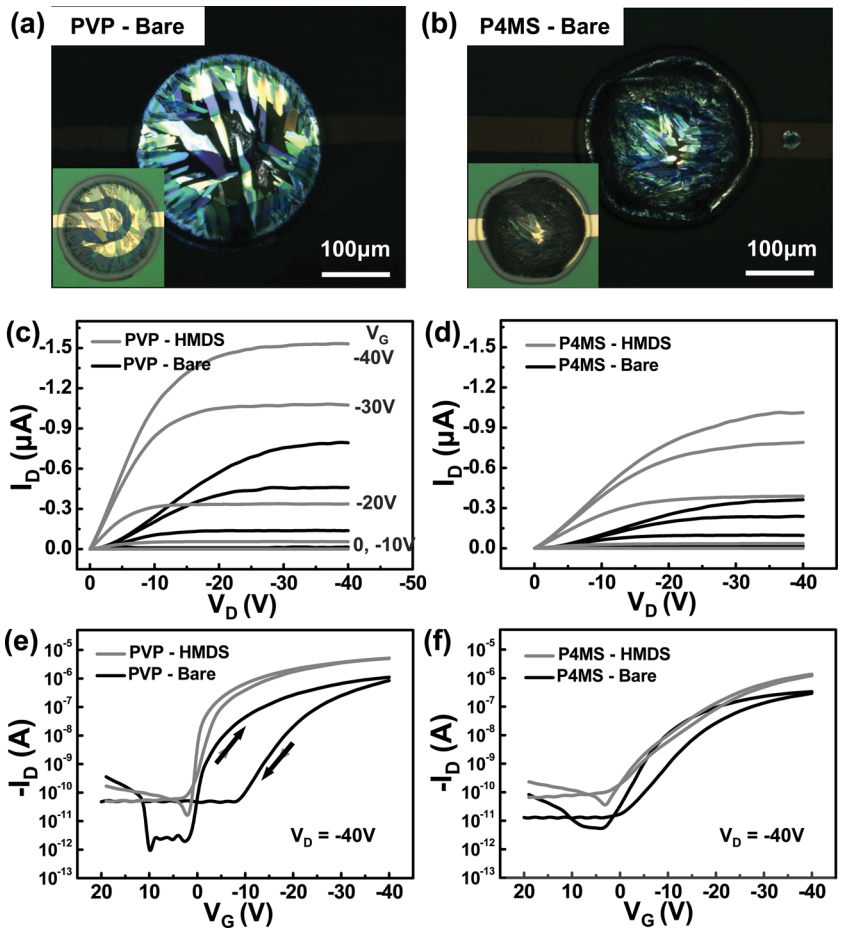

Figure 5. Polarized OM images of the TIPS-PEN devices prepared using each type of microwell: a) PVP and b) P4MS. The OM images obtained without polarized light are shown in the inset. The output and transfer characteristics of the devices prepared from the c,e) PVP microwell and d,f) P4MS microwell. In the output curves, V_G changed from 0 V to −40 V in increments of −10 V.

successful deposition of a semiconducting layer on a hydrophobic substrate is important. In a hydrophobic P4MS microwell, on the other hand, the TIPS_PEN crystals were relatively small and the birefringence of the crystals was weaker than that of crystals prepared in the PVP microwells (Figure 5b). Device performances were analyzed based on the output and transfer characteristics of the FETs prepared on surfaces submitted to different treatments. The electrical properties, including the average field-effect mobilities, on-off current ratios, threshold voltages, and subthreshold slopes, are summarized in **Table 2**.

Table 2. Electrical properties of transistors prepared using inkjet-printed TIPS_PEN films formed in each type of microwell-patterned bank.

Dielectric	Microwell	Mobility [$cm^2 V^{-1} s^{-1}$]	I_{on}/I_{off}	ΔV_{th} [V]	Subthreshold Swing [V/decade]
Bare	PVP	0.02 ± 0.01	1×10^6	13.7	1 ± 0.5
	P4MS	0.009 ± 0.003	5×10^4	7.2	3.9 ± 0.2
HMDS	PVP	0.1 ± 0.03	5×10^5	2.3	0.6 ± 0.3
	P4MS	0.04 ± 0.005	5×10^4	~0	3.5 ± 0.2

Both the saturation currents and the average field-effect mobilities for semiconducting layers prepared in the PVP microwells were twice the values obtained for semiconducting layers prepared in the P4MS microwells. This behavior arose from the highly crystalline TIPS_PEN crystals fabricated in the hydrophilic PVP microwells. The hydrophilic microwell induced preferential nucleation of the TIPS_PEN molecules at the top of the bank whereas the hydrodynamic flow induced cofacial stacking of the molecules with strong intermolecular π–π interactions. The TFTs prepared on the Bare-dielectric exhibited considerable hysteresis upon application of a dual V_G swing, whereas the hysteresis of the devices based on the HMDS-dielectric was greatly reduced (Figure 5e,f). Other device parameters obtained from the HMDS-dielectric were much better than those obtained from the Bare-dielectric. Thus, appropriate passivation of the SiO_2 dielectric surface using a hydrophobic organic layer was indispensable for improving the performances of OFET devices. Our study revealed that high-performance inkjet-printed transistors may be obtained by the development of self-assembled organic semiconductor crystals on hydrophobic dielectric surfaces using hydrophilic microwells.

3. Conclusions

In conclusion, we demonstrated a facile patterning technique for fabricating microwells by inkjet printing solvent drops on a polymer layer. Inkjet printing was then used to deposit organic semiconductor ink onto the prepatterned microwell banks to produce regular organic semiconductor deposits with a high accuracy. This technique is suitable for patterning organic semiconductor deposits on large-area flexible substrates, which is an expensive and complicated process using conventional photolithography.

We studied the influence of the surface wettability of a microwell on the evaporation and crystallization characteristics of inkjet-printed organic semiconductor droplets in the microwell. Inkjet-printed TIPS_PEN molecules self-organized to form highly ordered crystalline structures in the hydrophilic microwells as a result of contact line pinning at the top-corner of the microwell and the outward hydrodynamic flow within the drying droplet. By contrast, small crystallites with relatively poor molecular ordering formed in hydrophobic microwells because the contact line depinned along the wall of the microwells. The electrical properties of the resulting transistors were compared. The best performances were obtained from semiconductor crystals grown in the hydrophilic microwells. These results were well supported by the evaporation and crystallization characteristics of the organic semiconductor droplets

in the microwell. The hydrophilic microwell yielded highly ordered TIPS_PEN crystals on a hydrophobic dielectric surface, which should further increase the device performances.

4. Experimental Section

Materials: Poly(vinyl phenol) (PVP, Mw = 20 kg/mol) and poly(4-methyl styrene) (P4MS, Mw = 122 kg/mol) were purchased from Aldrich Chemical Co. 6,13-Bis(triisopropylsilylethynyl) pentacene (TIPS_PEN) was synthesized according to the procedure reported by Anthony and coworkers.[21]

Surface Modification of the Dielectric Layer: The silicon wafers were cleaned in piranha solution (70 vol% H_2SO_4 + 30 vol% H_2O_2) for 30 min at 100 °C then washed with distilled water. A bare hydrophilic surface was obtained by applying UV-ozone treatment for 20 min. The compound 1,1,1,3,3,3-hexamethyldisilazane (HMDS) (Aldrich, 99.9%) was spin-coated (3000 rpm, 60 s) onto a cleaned substrate then baked at 150 °C for 1 h. After baking, the sample was cleaned by ultrasonication in toluene, rinsed thoroughly with ethanol, and dried under vacuum.

Inkjet Printing System: A home-built inkjet printer incorporating a piezoelectric inkjet head (Microfab Jet Drive III), a two-axis motorized positioning system, and a charge-coupled device (CCD) camera aligned with a light-emitting diode (LED) were used to visualize the droplet ejection during the fabrication of the polymer banks and during the deposition of the TIPS-PEN. Single droplets with volumes of about 50 pL were ejected on demand from the nozzle, which had a diameter of 50 μm. The vertical separation between the nozzle and the substrate was typically 0.5 mm. The substrate was maintained under ambient conditions (26 °C, 30% humidity).

Microwell Formation by Inkjet Printing: Poly(melamine-co-formaldehyde) (PMF) and divinylbenzene were used as the cross-linking agents for the PVP and P4MS, respectively. PVP and PMF (or P4MS (hydrophobic material) and divinylbenzene) were dissolved in propylene glycol methyl ether acetate (PGMEA) to a concentration of 15 wt% (or in toluene to a concentration of 8 wt%), with a mole ratio of 1:1. The polymer films were formed by spin-coating the prepared solutions at 3000 rpm onto the surface-modified Si wafers. The microwell structure of the polymer bank was fabricated by repeatedly inkjet printing ethanol (or toluene) droplets over a given position. This solvent was a good solvent for PVP (or P4MS) and completely removed the PVP (or P4MS) layer. Finally, the PVP (or P4MS) film was cross-linked for 1 h at 180 °C in a vacuum oven (or under UV irradiation in a vacuum chamber) to yield a film that would be stable under the organic semiconductor inkjet printing process. The thickness of the cross-linked polymer film was about 350 nm in both cases.

Inkjet Printing of TIPS-PEN: A 1 wt% TIPS_PEN solution in tetralin (Fluka) was inkjet-printed onto the pre-patterned polymer microwells. The evaporation properties of the TIPS_PEN droplet were investigated using a charge-coupled device (CCD) (0.06 s/frame) until the solutions that had been deposited in the microwells were completely dry.

Fabrication of the OTFTs: TFTs with bottom-contact structures were fabricated using heavily doped n-type Si wafers as gate electrodes and a 300 nm thick thermally oxidized SiO_2 layer (capacitance = 10.8 nF/cm^2) as the gate dielectric. Conventional photolithography was used to deposit gold source and drain (S/D) electrodes in a structured closed-ring layout. The channel length-to-width (L/W) ratios were 30/300 (μm/μm). A 3-nm-thick titanium layer provided adhesion for the gold electrodes. Prior to depositing the TIPS_PEN solution by inkjet printing, the dielectric layer surfaces were modified and the microwells were fabricated at the position of the S/D electrodes as described above.

Characterization: The morphologies of the microwells and the TIPS-PEN deposits were characterized by optical microscopy (Axioplan, Zeiss) and field-emission scanning electron microscopy (Hitachi S-4800). The thicknesses and surface profiles of the polymer microwells were determined using an ellipsometer (M-200 V, H. A. Woollam) and a surface profiler (Alpha-Step 500), respectively. Two-dimensional grazing-incidence X-ray diffraction (2D-GIXD) and normal mode X-ray diffraction (XRD) measurements were performed at the 4C2 and 10B beamlines at the Pohang Accelerator Laboratory in Korea to study the molecular orientations in the TIPS-PEN films. The electrical properties of the transistors were characterized by measuring their current–voltage (I–V) curves (Keithley 2400 and 236 source/measure units) under ambient conditions. The field-effect mobilities (μ) and threshold voltages (V_{th}) of the TFT devices were calculated in the saturation regime (V_{DS} = –40 V) by plotting the square root of the drain current (I_{sd}) versus the gate voltage (V_g) using the following equation:

$$I_{sd} = \frac{WC_i}{2L}\mu \left(V_g - V_{th}\right)^2$$

where C_i (10.8 nF/cm^2) is the capacitance of the dielectric layer, and W and L are the channel width and length, respectively.

Supporting Information

Supporting Information is available from the Wiley Online Library or from the author.

Acknowledgements

This work was supported by a grant (Code No. 2011–0031628) from the Center for Advanced Soft Electronics under the Global Frontier Research Program of the Ministry of Science, ICT and Future Planning, Korea.

Received: March 15, 2013
Revised: April 19, 2013
Published online: June 5, 2013

[1] B. Kang, W. H. Lee, K. Cho, *ACS Appl. Mater. Interfaces* **2013**, *5*, 2302.
[2] M. Baklar, P. H. Wobkenberg, D. Sparrowe, M. Goncalves, I. McCulloch, M. Heeney, T. Anthopoulos, N. Stingelin, *J. Mater. Chem.* **2010**, *20*, 1927.
[3] J. A. Lim, W. H. Lee, H. S. Lee, J. H. Lee, Y. D. Park, K. Cho, *Adv. Funct. Mater.* **2008**, *18*, 229.
[4] S. Lim, B. Kang, D. Kwak, W. H. Lee, J. A. Lim, K. Cho, *J. Phys. Chem. C* **2012**, *116*, 7520.
[5] J. A. Lim, J. H. Kim, L. Qiu, W. H. Lee, H. S. Lee, D. Kwak, K. Cho, *Adv. Funct. Mater.* **2010**, *20*, 3292.
[6] H. Sirringhaus, T. Kawase, R. H. Friend, T. Shimoda, M. Inbasekaran, W. Wu, E. P. Woo, *Science* **2000**, *290*, 2123.
[7] M. Ikagawa, I. Tohno, T. Shinmura, S. Takagi, Y. Kataoka, M. Fujihira, *Jpn. J. Appl. Phys.* **2008**, *47*, 8935.
[8] T. Kawase, H. Sirringhaus, R. H. Friend, T. Shimoda, *Adv. Mater.* **2001**, *13*, 1601.
[9] Y. J. Xia, R. H. Friend, *Appl. Phys. Lett.* **2007**, *90*, 253513.
[10] S. R. Forrest, *Nature* **2004**, *428*, 911.
[11] Y. D. Park, J. A. Lim, H. S. Lee, K. Cho, *Mater. Today* **2007**, *10*, 46.
[12] P. C. Chang, J. Lee, D. Huang, V. Subramanian, A. R. Murphy, J. M. J. Frechet, *Chem. Mater.* **2004**, *16*, 4783.
[13] M. Ikegawa, H. Azuma, *JSME Int. J., Ser. B* **2004**, *47*, 490.
[14] M. Kaneda, H. Ishizuka, Y. Sakai, J. Fukai, S. Yasutake, *AIChE J.* **2007**, *53*, 1100.
[15] B. J. de Gans, U. S. Schubert, *Langmuir* **2004**, *20*, 7789.
[16] J. Park, J. Moon, *Langmuir* **2006**, *22*, 3506.
[17] E. Tekin, P. J. Smith, S. Hoeppener, A. M. J. van den Berg, A. S. Susha, A. L. Rogach, J. Feldmann, U. S. Schubert, *Adv. Funct. Mater.* **2007**, *17*, 23.

[18] J. A. Lim, J. H. Cho, Y. D. Park, D. H. Kim, M. Hwang, K. Cho, *Appl. Phys. Lett.* **2006**, *88*, 082102.
[19] K. Uno, K. Hayashi, T. Hayashi, K. Ito, H. Kitano, *Colloid Polym. Sci.* **1998**, *276*, 810.
[20] J. A. Lim, W. H. Lee, D. Kwak, K. Cho, *Langmuir* **2009**, *25*, 5404.
[21] J. E. Anthony, J. S. Brooks, D. L. Eaton, S. R. Parkin, *J. Am. Chem. Soc.* **2001**, *123*, 9482.
[22] D. H. Kim, D. Y. Lee, H. S. Lee, W. H. Lee, Y. H. Kim, J. I. Han, K. Cho, *Adv. Mater.* **2007**, *19*, 678.
[23] W. H. Lee, D. H. Kim, Y. Jang, J. H. Cho, M. Hwang, Y. D. Park, Y. H. Kim, J. I. Han, K. Cho, *Appl. Phys. Lett.* **2007**, *90*, 132106.
[24] B. J. de Gans, S. Hoeppener, U. S. Schubert, *Adv. Mater.* **2006**, *18*, 910.
[25] B. J. de Gans, S. Hoeppener, U. S. Schubert, *J. Mater. Chem.* **2007**, *17*, 3045.
[26] I. A. Grimaldi, A. D. Del Mauro, G. Nenna, F. Loffredo, C. Minarini, F. Villani, *J. Appl. Polym. Sci.* **2011**, *122*, 3637.
[27] H. C. Yang, T. J. Shin, M. M. Ling, K. Cho, C. Y. Ryu, Z. N. Bao, *J. Am. Chem. Soc.* **2005**, *127*, 11542.
[28] C. T. Chen, C. C. Chieng, F. G. Tseng, *J. Microelectromech. Syst.* **2007**, *16*, 1209.
[29] S. M. Rowan, M. I. Newton, G. Mchale, *J. Phys. Chem.* **1995**, *99*, 13268.
[30] H. Y. Erbil, G. McHale, M. I. Newton, *Langmuir* **2002**, *18*, 2636.
[31] C. W. Sele, B. K. C. Kjellander, B. Niesen, M. J. Thornton, J. B. P. H. van der Putten, K. Myny, H. J. Wondergem, A. Moser, R. Resel, A. J. J. M. van Breemen, N. van Aerle, P. Heremans, J. E. Anthony, G. H. Gelinck, *Adv. Mater.* **2009**, *21*, 4926.
[32] A. J. Kinloch, *Adhesion and Adhesives: Science and Technology*, Chapman and Hall, London/New York **1987**.